[1]H. Haken, *Synergetics* (Springer, Berlin, 1978).
[2]E. Schrödinger, Phys. Z. 16, 289 (1915); H. A. Kramers, Physica (Utrecht) 7, 284 (1940); D. A. Darling and A. J. F. Siegert, Ann. Math. Statist. 24, 624 (1953); E. W. Montroll and K. E. Schuler, Adv. Chem. Phys. 1, 361 (1958); R. Landauer and J. A. Swanson, Phys. Rev. 121, 1668 (1961).
[3]R. L. Stratonovich, *Topics in the Theory of Random Noise* (Gordon and Breach, New York, 1963), Vol. I, Chap. 4; G. H. Weiss, in *Stochastic Processes in Chemical Physics*, edited by I. Oppenheim, K. E. Schuler, and G. H. Weiss (MIT, Cambridge, Mass., 1977), p. 361.
[4]H. Risken and H. D. Vollmer, Z. Phys. 201, 323 (1967); M. O. Scully and W. E. Lamb, Jr., Phys. Rev. 159, 208 (1967); R. D. Hempstead and M. Lax, Phys. Rev. 161, 350 (1967); Y. K. Wang and W. E. Lamb, Jr., Phys. Rev. A 8, 873 (1973).
[5]M. M-Tehrani and L. Mandel, Phys. Rev. A 17, 677 (1978); F. T. Hioe, Surendra Singh, and L. Mandel, Phys. Rev. A 19, 2036 (1979).
[6]Surendra Singh and L. Mandel, Phys. Rev. A 20, 2459 (1979).
[7]L. Mandel, Rajarshi Roy, and Surendra Singh, in Optical Bistability, edited by C. M. Bowden, M. Ciftan, and H. Robl (Plenum, New York, to be published).
[8]A. Politi, Lett. Nuovo Cimento 27, 535 (1980); F. T. Arecchi and A. Politi, to be published.
[9]J. A. Abate, H. J. Kimble, and L. Mandel, Phys. Rev. A 14, 788 (1976).
[10]M. Sargent, III, M. O. Scully, and W. E. Lamb, Jr., *Laser Physics* (Addison-Wesley, Reading, Mass., 1974).

# Efficiency Factors in Mie Scattering

H. M. Nussenzveig[(a)]
*Cooperative Institute for Research in the Environmental Sciences, Boulder, Colorado 80309, and National Center for Atmospheric Research, Boulder, Colorado 80307*

and

W. J. Wiscombe
*National Center for Atmospheric Research, Boulder, Colorado 80307*
(Received 22 May 1980)

Asymptotic approximations to the Mie efficiency factors for extinction, absorption, and radiation pressure, derived from complex-angular-momentum theory and averaged over $\Delta\beta \sim \pi$ ($\beta$ = size parameter), are given and compared with the exact results. For complex refractive indices $N = n + i\kappa$ with $1.1 \leq n \leq 2.5$ and $0 \leq \kappa \leq 1$, the relative errors decrease from ~(1–10)% to ~($10^{-2}$–$10^{-3}$)% between $\beta = 10$ and $\beta = 1000$, and computing time is reduced by a factor of order $\beta$, so that the Mie formulae can advantageously be replaced by the asymptotic ones in most applications.

PACS numbers: 42.20.Gg, 42.68.Vs

The Mie efficiency factors[1] for extinction ($Q_{ext}$), absorption ($Q_{abs}$), and radiation pressure ($Q_{pr}$) are just the corresponding cross sections divided by the projected area $\pi a^2$ of the scattering sphere. These quantities are important in many applications. Typical size parameters $\beta = ka$ ($k$ = wave number, $a$ = droplet radius) range from $\ll 1$ up to $\sim 10^4$, with complex refractive indices $N = n + i\kappa$, $1.1 \lesssim n \lesssim 1.9$, $10^{-9} \lesssim \kappa \lesssim 1$. The efficiencies vary extremely rapidly[2] with $\beta$, $n$ and $\kappa$; but in most applications one is only interested in means $\langle Q \rangle$ over some range $\Delta\beta$, not in this high-frequency "ripple."

Evaluation of the exact Mie expressions[1] requires summing $\sim \beta$ partial waves. Upon integration across size or wavelength with a step fine enough to resolve the ripple ($\Delta\beta \leq 0.01$–$0.1$), one is faced with exorbitant computation times. Approximations[1] based on geometrical optics and classical diffraction theory do not have the required accuracy until $\beta$ exceeds several thousand (cf. below). Clearly, better approximations, devoid of ripple, are needed.

The complex-angular-momentum theory of Mie scattering[3] can furnish such approximations. By a simple extension of previously developed techniques,[4,5] we find for the extinction efficiency,

$$Q_{\text{ext}} = 2 + 1.992\,386\,1\beta^{-2/3} + 8\,\text{Im}\Big\{\tfrac{1}{4}(N^2+1)(N^2-1)^{-1/2}\beta^{-1} - N^2(N+1)^{-1}(N^2-1)^{-1}\Big[1+\frac{i}{2\beta}\Big(\frac{1}{N-1}-\frac{N-1}{N}\Big)\Big]\beta^{-1}$$
$$\times\exp[2i(N-1)\beta] - \tfrac{1}{2}(N-1)\sum_{j=1}^{\infty}\Big[j-\Big(\frac{N-1}{2}\Big)\Big]^{-1}\Big(\frac{N-1}{N+1}\Big)^{2j}$$
$$\times\exp[2i(N-1+2jN)\beta]\Big\} - 0.715\,353\,7\beta^{-4/3} - 0.332\,064\,3$$
$$\times\,\text{Im}[e^{i\pi/3}(N^2-1)^{-3/2}(N^2+1)(2N^4-6N^2+3)]\beta^{-5/3} + O(\beta^{-2}) + \text{ripple}. \quad (1)$$

To obtain the average absorption efficiency $\langle Q_{\text{abs}}\rangle$ over $\Delta\beta\sim\pi$, one applies the modified Watson transformation[3] to the corresponding Mie series expansion[1,2] and then takes the average over $\Delta\beta$. The result[6] is

$$\langle Q_{\text{abs}}\rangle = \langle Q_{\text{abs}}\rangle_F + \langle Q_{\text{abs}}\rangle_{\text{a.e.}} + \langle Q_{\text{abs}}\rangle_{\text{b.e.}}, \quad (2)$$

$$\langle Q_{\text{abs}}\rangle_F = \sum_{\lambda=1}^{2}\int_0^{\pi/2}\varphi(r_{j\lambda})\sin\theta\cos\theta\,d\theta, \quad (3)$$

$$\langle Q_{\text{abs}}\rangle_{\text{a.e.}} = 2^{-1/3}\beta^{-2/3}\sum_{\lambda=1}^{2}\int_0^{x_a}\varphi(r_{j\lambda}{}^{+})\,dx, \quad (4)$$

$$\langle Q_{\text{abs}}\rangle_{\text{b.e.}} = 2^{-1/3}\beta^{-2/3}\sum_{\lambda=1}^{2}\int_0^{x_b}[\varphi(r_{j\lambda}{}^{-}) - \varphi(\tilde{r}_{j\lambda}{}^{-})]\,dx, \quad (5)$$

where

$$\varphi(r_{j\lambda}) = (1-e^{-b})(1-r_{2\lambda})/(1-r_{1\lambda}e^{-b}), \quad (6)$$

and $r_{2\lambda}$ and $r_{1\lambda}$ are, respectively, the external and internal reflectivities for polarization $\lambda$, given by

$$r_{j\lambda} = |R_{j\lambda}|^2, \quad j,\lambda = 1,2; \quad R_{j\lambda} = (-1)^j(z_j - ue_\lambda)/(z+ue_\lambda); \quad (7)$$

$$z = \cos\theta, \quad u = N\cos\theta', \quad \sin\theta = N\sin\theta', \quad (8)$$

$$e_1 = 1, \quad e_2 = N^{-2}, \quad z_1 = z, \quad z_2 = \begin{cases} z \text{ for Eq. (3)} \\ z^* \text{ for Eqs. (4) and (5)}, \end{cases}$$

and

$$b = 4\beta\,\text{Im}(N\cos\theta' + \theta'\sin\theta). \quad (9)$$

$\theta'$ is the *complex* angle of refraction corresponding to the angle of incidence $\theta$. [(8) is just Snell's Law.] $r_{j\lambda}$ are the Fresnel reflectivities ($r_{2\lambda} = r_{1\lambda}$), and $b$ is the damping exponent along a *complex* shortcut through the sphere. Thus (3) is an improved version of the geometrical-optic[1] result.

The terms (4) and (5) represent the contribution from the edge domain[3] (a.e. = above edge; b.e. = below edge); $r_{j\lambda}{}^{\pm}$ is obtained from $r_{j\lambda}$ by the substitution

$$z \to z^{\pm} = -(2/\beta)^{1/3}e^{i\pi/6}\text{Ai}'(\pm xe^{2i\pi/3})/\text{Ai}(\pm xe^{2i\pi/3}), \quad (10)$$

where Ai is the Airy function, $\theta$ is related to $x$ by

$$\sin\theta = 1 \pm 2^{-1/3}\beta^{-2/3}x \quad (+\text{ in a.e.}; -\text{ in b.e.}) \quad (11)$$

[with corresponding changes in the derived quantities (8) and (9)], and the limits of integration are

$$x_a = 2^{1/3}(n-1)\beta^{2/3}, \quad x_b = (\beta/2)^{2/3}. \quad (12)$$

Finally, in (5), $\tilde{r}_{j\lambda}{}^{-}$ is obtained from $r_{j\lambda}{}^{-}$ by the substitution

$$z^{-} \to (2/\beta)^{1/3}x^{1/2}. \quad (13)$$

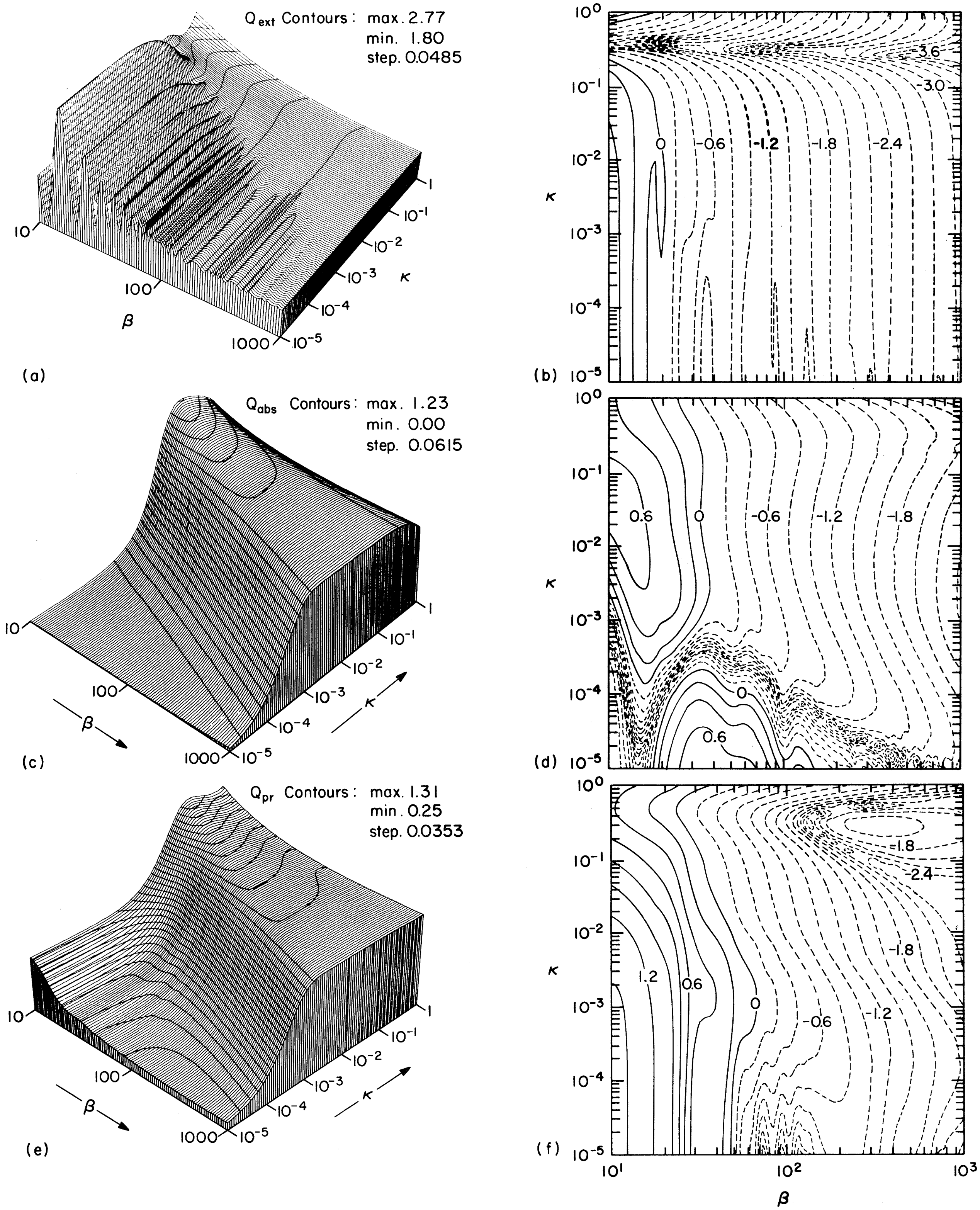


FIG. 1. (a) Three-dimensional plot of $\langle Q_{ext}\rangle$ for $n=1.33$, $10^{-5}\leq\kappa\leq 1$, $10\leq\beta\leq 10^{3}$. The numbers attached to surface represent values of $\langle Q_{ext}\rangle$. (b) Level curves for the logarithm of the percentage errors of the asymptotic approximation to $\langle Q_{ext}\rangle$. Negative values (errors < 1%) are shown by dotted lines. (c) Same as (a) for $\langle Q_{abs}\rangle$. (d) Same as (b) for $\langle Q_{abs}\rangle$. (e) Same as (a) for $\langle Q_{pr}\rangle$. (f) Same as (b) for $\langle Q_{pr}\rangle$.

The average radiation-pressure efficiency is given by[6]

$$\langle Q_{\mathrm{pr}}\rangle = 1 - \langle w_g\rangle_F - \langle w_g\rangle_{\mathrm{a.e.}} - \langle w_g\rangle_{\mathrm{b.e.}}, \tag{14}$$

$$\langle w_g\rangle_F = \mathrm{Re}\sum_{\lambda=1}^{2}\int_0^{\pi/2} d\theta\,\sin\theta\,\cos\theta\, e^{-2i\theta}[-|R_{2\lambda}|^2 + |1-(R_{2\lambda})^2|^2(1+f_2|R_{1\lambda}|^2 e^{-b})^{-1} f_2 e^{-b}], \tag{15}$$

$$\langle w_g\rangle_{\mathrm{a.e.}} = 2^{-1/3}\beta^{-2/3}\,\mathrm{Re}\sum_{\lambda=1}^{2}\int_0^{x_a}(\rho_\lambda^{+} - \tau_\lambda^{+} + 1)\,dx, \tag{16}$$

$$\langle w_g\rangle_{\mathrm{b.e.}} = 2^{-1/3}\beta^{-2/3}\,\mathrm{Re}\sum_{\lambda=1}^{2}\int_0^{x_b}[(\rho_\lambda^{-} - \hat\rho_\lambda^{-}) - (\tau_\lambda^{-} - \hat\tau_\lambda^{-})]\,dx, \tag{17}$$

where

$$\rho_\lambda = f_1(z) R_{2\lambda}{}^* R_{2\lambda}{}', \tag{18}$$

$$\tau_\lambda = f_1(z) f_2 e^{-b}(1+R_{1\lambda}{}^*)(1+R_{1\lambda}{}')(1+R_{2\lambda}{}^*)(1+R_{2\lambda}{}')(1+R_{1\lambda}{}^* R_{1\lambda}{}' f_2 e^{-b})^{-1}, \tag{19}$$

$$f_1(z) = (1+iz^*)/(1-iz), \quad f_2 = e^{-2i\theta'}, \tag{20}$$

$$R_{j1}{}' = (f_j)^{-1}[N^2 z_j - u + (-1)^j iM^2](N^2 z + u + iM^2)^{-1}, \tag{21}$$

$$R_{j2}{}' = (f_j)^{-1}[(N^2+M^2) z_j - u + (-1)^j iM^2(1-uz_j)][(N^2+M^2)z + u + iM^2(1+uz)]^{-1}, \tag{22}$$

with $M^2 = N^2 - 1$. In all quantities with $(\pm)$ upper indices, the substitutions (10) and (11) are understood. Finally, $\hat\rho_\lambda^{-}$ and $\hat\tau_\lambda^{-}$ are obtained from $\rho_\lambda^{-}, \tau_\lambda^{-}$ by the substitution

$$z^{-} \to (2/\beta)^{1/3}(\sqrt{x} + i/4x). \tag{23}$$

Again, (15) represents an improved version of the geometrical-optic[7] result, while (16) and (17) represent above-edge and below-edge corrections.

We have made detailed comparisons[6] between the exact Mie results (suitably averaged to eliminate the ripple[8]) and the above asymptotic approximations[9] over the ranges $10 \leqslant \beta \leqslant 5000$, $0 \leqslant \kappa \leqslant 1$, for $n = 1.10$, 1.33, 1.50, 1.90, and 2.50. Results for $n = 1.33$ and $10 \leqslant \beta \leqslant 1000$ are shown in Fig. 1.

Figure 1(a) is a three-dimensional plot of $\langle Q_{\mathrm{ext}}\rangle$. The oscillations arise form interference between diffracted and transmitted light, and they are damped out as $\kappa\beta$ increases. Figure 1(b) shows level curves for the logarithm of the percentage error of approximation (1). Negative values (errors < 1%) are shown by dotted lines. Thus the relative error falls below 1% already at $\beta \gtrsim 15$, it is $\lesssim 0.1\%$ at $\beta \gtrsim 70$, $\lesssim 0.01\%$ at $\beta \gtrsim 200$, and $\lesssim 10^{-3}\%$ at $\beta \gtrsim 10^3$.

Figures 1(c) and 1(d) show similar plots for $\langle Q_{\mathrm{abs}}\rangle$, and Figs. 1(e) and 1(f) for $\langle Q_{\mathrm{pr}}\rangle$. The relative errors are somewhat greater than for $\langle Q_{\mathrm{ext}}\rangle$ and are the worst for $\langle Q_{\mathrm{pr}}\rangle$, where one must have $\beta \geqslant 90$ to achieve better than 1% error.

The accuracy improves not only as $\beta$ increases, but also as $n$ increases. Previously known approximations (based on geometrical optics and classical diffraction theory) have an accuracy that is almost independent of $n$ and that only reaches 1% at $\beta = 1000$ and (0.2–0.5)% at $\beta = 5000$.

The computing time is reduced relative to exact Mie computations roughly by a factor of $O(\beta)$, and it is only about twice that for geometrical-optic approximations.

Besides the improvement to the geometrical-optic–type contributions, the main asymptotic corrections arise from the edge domain. Their functional form is quite similar to the geometrical-optic one, extended to complex angles of incidence and refraction. Thus, as was found in previous discussions,[3] the edge effects represent a kind of analytic continuation of ray optics to complex paths, where diffraction corresponds to barrier penetration. Similar interpretations have been suggested in atomic,[10] nuclear,[11] and particle[12] physics.

The National Center for Atmospheric Research is sponsored by the National Science Foundation.

[a]Permanent address: Instituto de Fisica, Universidade de São Paulo, 01000 São Paulo, Brazil.

[1]H. C. van de Hulst, *Light Scattering by Small Particles* (Wiley, New York, 1957).

[2]W. M. Irvine, J. Opt. Soc. Am. 55, 16 (1965).

[3]Cf. H. M. Nussenzveig, J. Opt. Soc. Am. 69, 1068 (1979), and references therein.

[4]H. M. Nussenzveig, J. Math. Phys. 10, 82, 125 (1969).

[5]V. Khare, Ph.D. thesis, University of Rochester, 1975 (unpublished).

[6]H. M. Nussenzveig and W. J. Wiscombe, to be published.

[7]P. J. Debye, Ann. Phys. 30, 57 (1909).

[8]The Mie computations were performed using algorithms of Wiscombe [Appl. Opt. 19, 1505 (1980)]. High-frequency ripple was removed from the Mie data by least-squares quartic spline fitting with knots every $\Delta\beta \sim 10$ for $Q_{abs}$ and $Q_{pr}$, and by low-pass filtering for $Q_{ext}$.

[9]A fairly well-tested set of computer routines for calculating Eqs. (1), (2), and (14) is available from one of us (W.J.W.) upon request.

[10]J. N. L. Connor and W. Jakubetz, Mol. Phys. 35, 949 (1978); S. Bosanac, Mol. Phys. 35, 1057 (1978).

[11]R. C. Fuller and P. J. Moffa, Phys. C 15, 266 (1977).

[12]B. Schrempp and F. Schrempp, Phys. Lett. 70B, 88 (1977); Centre Européen de Recherches Nucléaires Report No. CERN-TH 2573, 1978 (to be published).

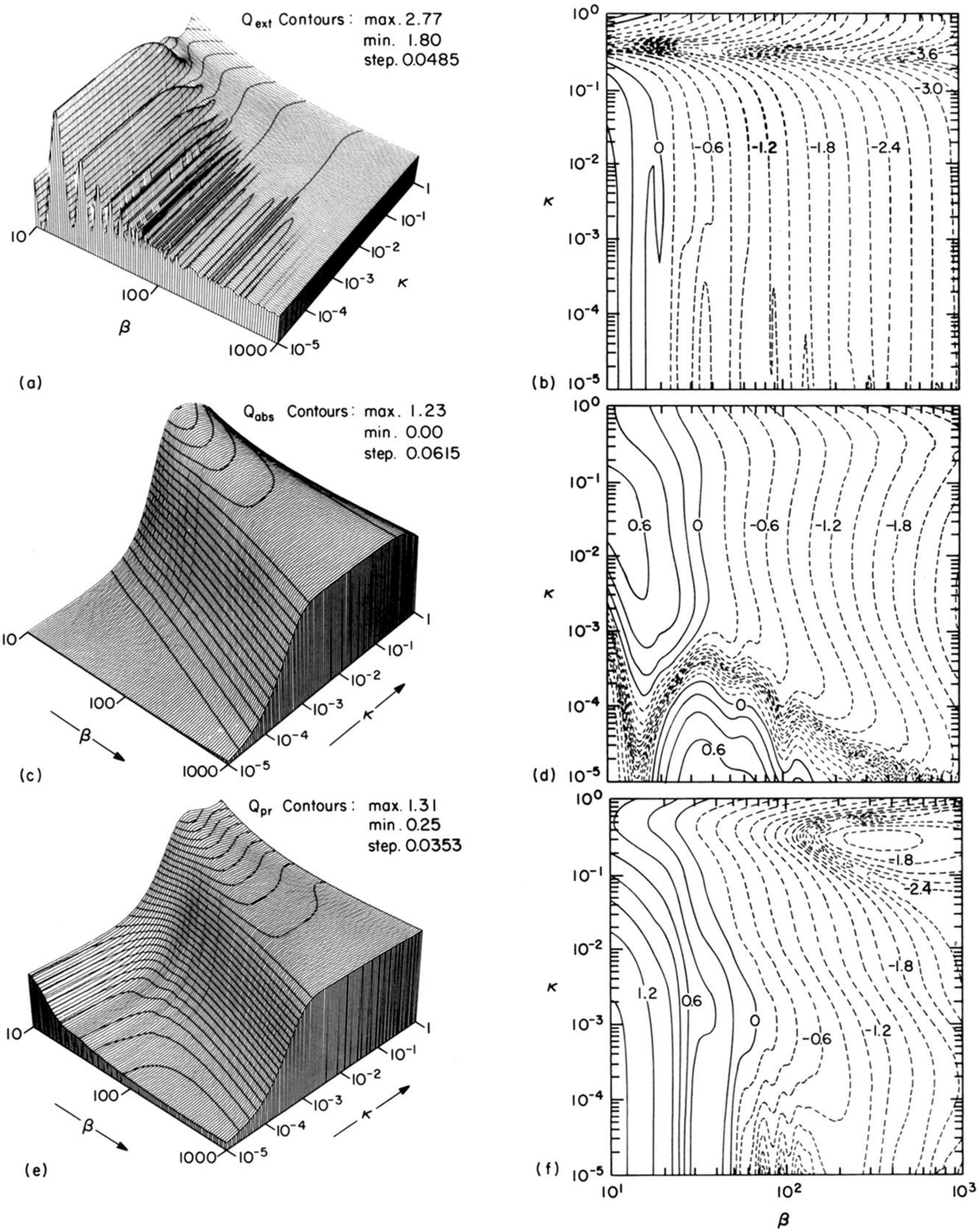


FIG. 1. (a) Three-dimensional plot of $\langle Q_{\rm ext}\rangle$ for $n=1.33$, $10^{-5}\leq\kappa\leq1$, $10\leq\beta\leq10^3$. The numbers attached to surface represent values of $\langle Q_{\rm ext}\rangle$. (b) Level curves for the logarithm of the percentage errors of the asymptotic approximation to $\langle Q_{\rm ext}\rangle$. Negative values (errors < 1%) are shown by dotted lines. (c) Same as (a) for $\langle Q_{\rm abs}\rangle$. (d) Same as (b) for $\langle Q_{\rm abs}\rangle$. (e) Same as (a) for $\langle Q_{\rm pr}\rangle$. (f) Same as (b) for $\langle Q_{\rm pr}\rangle$.